JOURNAL OF VIROLOGY, Oct. 2011, p. 10375–10388 Vol. 85, No. 19
0022-538X/11/$12.00 doi:10.1128/JVI.00226-11

Deletion of Kaposi's Sarcoma-Associated Herpesvirus FLICE Inhibitory Protein, vFLIP, from the Viral Genome Compromises the Activation of STAT1-Responsive Cellular Genes and Spindle Cell Formation in Endothelial Cells[▽]

Khaled R. Alkharsah,[1]† Vivek Vikram Singh,[1]† Raffaella Bosco,[1,5] Susann Santag,[1] Adam Grundhoff,[3] Andreas Konrad,[4] Michael Stürzl,[4] Dagmar Wirth,[6] Oliver Dittrich-Breiholz,[2] Michael Kracht,[7] and Thomas F. Schulz[1]*

Institute of Virology, Hannover Medical School, Hannover, Germany[1]; Institute of Biochemistry, Hannover Medical School, Hannover, Germany[2]; Heinrich Pette Institute, Hamburg, Germany[3]; Department of Surgery, Division of Molecular and Experimental Surgery, University of Erlangen-Nuremberg, Erlangen, Germany[4]; Department of Oncology, Hematology, and Respiratory Diseases, University of Modena and Reggio Emilia, Modena, Italy[5]; Department of Gene Regulation and Differentiation, Helmholtz Centre for Infection Research, Braunschweig, Germany[6]; and Rudolf Buchheim Institute of Pharmacology, Justus Liebig University Giessen, Giessen, Germany[7]

Received 1 February 2011/Accepted 7 July 2011

Kaposi's sarcoma herpesvirus (KSHV) Fas-associated death domain (FADD)-like interleukin-1 beta-converting enzyme (FLICE)-inhibitory protein, vFLIP, has antiapoptotic properties, is a potent activator of the NF-κB pathway, and induces the formation of endothelial spindle cells, the hallmark of Kaposi's sarcoma, when overexpressed in primary endothelial cells. We used a reverse genetics approach to study several functions of KSHV vFLIP in the context of the whole viral genome. Deletion of the gene encoding vFLIP from a KSHV genome cloned in a bacterial artificial chromosome (BAC) reduced the ability of the virus to persist and induce spindle cell formation in primary human umbilical vein endothelial cells (HUVECs). Only a few, mainly interferon (IFN)-responsive, genes were expressed in wild-type KSHV (KSHV-wt)-infected endothelial cells at levels higher than those in KSHV-ΔFLIP-infected endothelial cells, in contrast to the plethora of cellular genes induced by overexpressed vFLIP. In keeping with this observation, vFLIP induces the phosphorylation of STAT1 and STAT2 in an NF-κB-dependent manner in endothelial cells. vFLIP-dependent phosphorylation of STAT1 and STAT2 could be demonstrated after endothelial cells were infected with KSHV-wt, KSHV-ΔFLIP, and a KSHV-vFLIP revertant virus. These findings document the impact of KSHV vFLIP on the transcriptome of primary endothelial cells during viral persistence and highlight the role of vFLIP in the activation of STAT1/STAT2 and STAT-responsive cellular genes by KSHV.

Kaposi's sarcoma herpesvirus (KSHV), also called human herpesvirus 8 (HHV-8), was first detected in KS patient tissue (14) and is an indispensable factor in the development of this tumor (for a review, see reference 56). KSHV was found also to be associated with two other lymphoproliferative disorders, primary effusion lymphoma (12) and the plasma cell variant of multicentric Castleman's disease (57). Many groups have shown the ability of KSHV to infect primary endothelial cells *in vitro* and induce spindling morphology reminiscent of KS tumor cells (10, 18, 24, 26). Most spindle cells are latently infected with KSHV, and only a small proportion of them undergo spontaneous lytic replication. KSHV-infected endothelial cells exhibit a gene expression profile resembling that of lymphatic endothelial cells, and KSHV can reprogram infected vascular endothelial cells to express a lymphatic endothelial profile and *vice versa* (32, 67). The reprogrammed gene expression profile includes the upregulated expression of several specific lymphatic endothelial genes, including VEGFR3, podoplanin, LYVE1, and Prox-1, in dermal microvascular endothelial cells upon KSHV infection (11). The K13 latent viral gene (also referred to as open reading frame 71 [*orf71*]) encodes the Fas-associated death domain (FADD)-like interleukin-1 beta-converting enzyme (FLICE)-inhibitory protein (vFLIP). It has homology to cellular FLIP (cFLIP) (15, 63). Two predominant forms of cFLIP exist. $cFLIP_S$ (27) is the short form and contains only two N-terminal death effector domains (DEDs), which are very similar to the prodomains of caspase 8 and 10. The long splice variant of cFLIP ($cFLIP_L$) contains tandem N-terminal DEDs with an altered caspase domain that makes $cFLIP_L$ enzymically inactive (50). By virtue of their DEDs, cFLIPs block the interaction between FADD and procaspases 8 and 10, and this prevents receptor-mediated apoptosis (5, 63). KSHV vFLIP contains two homologous copies of the DED and is similar to the short form of its cellular homologue. In agreement with this predicted antiapoptotic activity of vFLIP, Sun et al. have shown the ability of vFLIP to protect against growth factor withdrawal-induced apoptosis in the growth factor-dependent TF-1 leukemia cell line but not against tumor necrosis factor alpha (TNF-α)-induced or anticancer drug-induced apoptosis (61). Downregulation of vFLIP

* Corresponding author. Mailing address: Institut für Virologie, Hannover Medical School, Carl-Neuberg Str. 1, D-30625 Hannover, Germany. Phone: 49-511-532-6736. Fax: 49-511-532-8736. E-mail: schulz.thomas@mh-hannover.de.
† These authors contributed equally to this work.
▽ Published ahead of print on 27 July 2011.

in primary effusion lymphoma cell lines led to induction of apoptosis and cell death (27, 31). In KS lesions, the expression of the vFLIP transcript was found to increase in late-stage lesions and was inversely correlated with apoptosis (58). However, thymocytes from a vFLIP-transgenic mouse showed a rate of cell death similar to that of the negative-control cells when induced with either anti-fibroblast cell line (FS-7)-associated surface antigen antibody (FAS-Ab) or dexamethasone, indicating the failure of vFLIP to block either the intrinsic or the extrinsic apoptosis pathway in this system (17). Recently, the role of vFLIP in the initiation of primary effusion lymphoma (PEL) and multicentric Castleman's disease, by specifically expressing vFLIP at different stages of B cell differentiation *in vivo*, was determined. The authors reported that vFLIP can induce B cell transdifferentiation (reprogramming), thereby promoting the emergence of B cell-derived tumors that display Ig gene rearrangements and a downregulated expression of B cell-associated antigens, thus resembling a PEL immunophenotype (3). Inhibition of detachment-induced apoptosis (anoikis) in dermal microvascular endothelial cells by vFLIP may contribute to KS oncogenesis by allowing the detachment and spread of single cells from one lesion (metastasis) (21). Recently, vFLIP was also shown to protect human umbilical vein endothelial cells (HUVECs) from superoxide-induced apoptosis by upregulating the expression of the manganese superoxide dismutase gene (MnSOD) (64).

Most of these activities are nuclear factor kappa B (NF-κB) dependent. KSHV vFLIP is unique among other viral FLIPs in its ability to activate both the canonical and the alternative NF-κB pathway (15, 41). It binds to IκB kinase gamma (IKK-γ) on the HLX2 domain and induces conformational changes leading to its autoactivation (2, 23). NF-κB activation seems to be central for vFLIP functions. Other than having the above-mentioned cell survival and antiapoptotic functions, vFLIP also induces cytokine secretions like interleukin-8 (IL-8) and CXCL16 in an NF-κB-dependent manner (60, 70). By an NF-κB-dependent mechanism, vFLIP was also shown to manipulate Notch signaling by upregulation of JAG1 gene expression, leading to the expression of Notch-responsive genes like HEY1 in vFLIP-expressing and neighboring lymphatic endothelial cells (22).

Furthermore, the NF-κB-dependent functions of vFLIP extend toward blocking KSHV lytic reactivation and virus production (72), most probably by inhibiting the replication transcription activator (RTA) promoter's activity through suppression of the AP-1 pathway (71). It was also demonstrated that vFLIP has a unique ability among other viral FLIPs to transform Rat-1 and BALB/3T3 fibroblast cells and to form tumors in nude mice. This ability was also NF-κB associated (61). In addition, overexpression of vFLIP in primary endothelial cells induces, again in an NF-κB-dependent manner, the formation of spindle cells, the hallmark of KS lesions (29). However, in the KSHV genome, vFLIP is translated from the second exon of a bicistronic mRNA that also encodes the viral cyclin homologue, vCyc, and is only weakly expressed at the protein level (38). To what extent the results obtained with overexpressed vFLIP reflect its role in the context of the entire viral genome is thus not clear. We therefore applied a reverse genetics approach to investigate several functions of vFLIP in the context of the whole viral genome. We deleted *orfK13*, the gene encoding vFLIP, from a KSHV genome cloned into a bacterial artificial chromosome (BAC) (73). We confirm the role of vFLIP in inducing spindle cell formation in primary endothelial cells. The absence of vFLIP from the viral genome affects the expression of only a few STAT-regulated genes during viral persistence, in contrast to the plethora of cellular genes that are modulated by overexpressed vFLIP. In keeping with this observation, we show that vFLIP expression induces the activation and phosphorylation of STAT1 and STAT2 in endothelial cells.

MATERIALS AND METHODS

Cells and transfections. HEK293 cells were grown in Dulbecco's modified Eagle's medium (DMEM) supplemented with 10% fetal bovine serum (HyClone, Germany), penicillin (100 U/ml), and streptomycin (100 μg/ml) (Cytogen, Germany). Vero cells were maintained in minimal essential medium (MEM) (Earle's balanced salt solution [BSS], nonessential amino acids [NEAA], L-glutamine, and 2.2 g/liter $NaHCO_3$) (Cytogen, Germany). HUVECs were isolated from freshly obtained human umbilical cords by collagenase digestion of the interior of the umbilical vein as described previously (33). HUVECs were cultured in the low-serum (5%) endothelial cell growth medium 2 for microvacular cells (EGM-2-MV) with its specific supplement (Lonza). An endothelial cell line, HuAR2T-tert, conditionally immortalized with doxycycline-dependent human telomerase reverse transcriptase (hTERT) and simian virus 40 (SV40) T antigen (TAg) transgene expression (43), was kindly provided by D. Wirth. HuAR2T-tert cells were maintained in EGM-2-MV medium in the presence of doxycycline at a concentration of 2 μg/ml. Transfection of HUVECs with small interfering RNA (siRNA) was done using the Neon transfection system according to the manufacturer's instructions (Invitrogen). One hundred picomoles of siRNA was microporated into 10^5 cells, which were then plated in one well of a 24-well plate. All siRNA oligonucleotides (siGENOME SMARTpool) for JAK1, JAK2, TYK2, RELA, IKBKG, and nontargeting siRNA pool no. 1 were purchased from Thermo Scientific (catalog no. M-003145-02-0005, M003146-02-0005, M-003182-02-0005, M-003533-02-0005, M-003767-02-0005, and D-001206-13-20, respectively).

Sf9 cells were maintained in Grace's medium supplemented with 10% fetal calf serum (FCS), penicillin (100 U/ml), and streptomycin (100 μg/ml) (Cytogen, Germany) and incubated at 28°C. The generation of the recombinant baculovirus expressing KSHV ORF50/RTA was described previously (66).

Antibodies. The following antibodies were used: mouse anti-latency-associated nuclear antigen (anti-LANA; 1:50; Novocastra) for the immunofluorescence assay, rat anti-LANA (1:2,000; ABI) for Western blotting, anti-green fluorescent protein (anti-GFP) antibody (Clontech), and anti-actin antibody (Chemicon). Anti-JAK2, -pJAK2 (Y1007/1008), -JAK1, -pJAK1 (Y1022/1023), -Tyk2, -pTyk2 (Y1054/1055), -STAT1, -pSTAT1 (Y701), -pSTAT1 (S727), -STAT2, -pSTAT2 (Y690), -STAT3, -pSTAT3 (Y705), -pSTAT3 (S727), -STAT5, -pSTAT5 (Y694), -STAT6, -pSTAT6 (Y641), and -IKK-γ antibodies were purchased from Cell Signaling. Anti-RelA (p65) and rat anti-hemagglutinin high-affinity (anti-HA) antibody were purchased from Santa Cruz Biotechnology and Roche, respectively. A rat monoclonal antibody to vFLIP (4C1) was kindly provided by E. Kremmer.

Plasmids. An *Escherichia coli* strain (DH10B) containing the KSHV genome cloned in a bacterial artificial chromosome (BAC36) was obtained from S. J. Gao (73). BAC-KSHV-ΔFLIP (KSHV-ΔFLIP) was generated from the BAC-KSHV wild type (KSHV-wt) by a RecE/Rect recombinant proteins cloning strategy (ET cloning) (see below). The pKD46 plasmid expressing the recombination enzymes under the L-arabinose-inducible promoter is described elsewhere (20). The *rpsL-neo* cassette carrying 61-bp homologous regions flanking vFLIP (*rpsL-neo* + homology cassette) was obtained by PCR using the following primers: vFLIP ko for, 5′-AGTGTTTATTAAATCAGATACATACATTCTACGGACCAAAAATTAGCAACAGCTTGTTATTCAGAAGAACTCGTCAAGAAGGCG-3′, and vFLIP ko rev, 5′-GAAAAATAAATTTTCCTTTGTTTTTCCACATCGGTGCCTTCACATATACAAGCCGGCACCGGCCTGGTGATGATGGCGGGATCG-3′. The parts of the primer that anneal in the pRpsL-neo plasmid (Gene Bridges, Germany) are underlined. The KSHV-ΔFLIP construct was electroporated into *E. coli* strain GS1783 to generate GS1783-KSHV-ΔFLIP. The following primers were used to generate the KSHV-FLIP revertant (KSHV-FLIP-R): sac isce zeo for, ATCTGAGCTCTAGGGATAACAGGGTAATTTTGTCTCCGCAGCTCCTGAG, sac fliph zeo rev, ATTGGAGCTCTTAGAGCTTTAAAGGAGGAGGGCAGGTTAACGTTTCCCCTGTTATCTGTGGATAACCGT

ATTACCG, VFLIP KIN FOR, AGTGTTTATTAAATCAGATACATACATT CTACGGACCAAAAATTAGCAACAGCTTGTTATCTATGGTGTATGGC GATAGTGTTG, and VFLIP KIN REV, GAAAAATAAATTTTCCTTTGTT TTTCCACATCGGTGCCTTCACATATACAAGCCGGCACCATGGCCACT TACGAGGTTCTCTG.

To construct a vFLIP-expressing lentiviral vector, the DNA fragment containing the vFLIP open reading frame was amplified from KSHV DNA (BAC36-wt) by PCR with the following primers: vFLIP NcoI, 5′-ATCTCCATGGCCACTT ACGAGGTTCTCTGT-3′, and vFLIP SalI, 5′-TTCTGTCGACTATGGTGTA TGGCGATAGTGTTGGGA-3′. The T2A element was amplified from a plasmid (kindly provided by A. Schambach) with the following primers: T2A BsrGI, 5′-TTGCTGTACAAGGGCTCCGGAGAGGGCCGGGGCTCTC-3′, and T2A NcoI, 5′-TCTGCCATGGAGGGGCCGGGGTTCTCCTCCACGT-3′. The amplified fragments were ligated and inserted into the lentiviral vector pRRL.PPT.SF.GFPpre (control vector) (kindly provided by A. Schambach) at the BsrGI and SalI sites to generate a lentiviral vFLIP vector. Another vFLIP construct tagged with HA at its C-terminal part (vFLIP-HA vector) was produced by PCR using the following primers: vFLIP NcoI and 3′vFLIPHA SalI, 5′TTCTGTCGACTAGGCGTAGTCGGGCACGTCGTAGGGGTATGGTGT ATGGCGATAGTGTTGGGA-3′, and cloned in the same vector. The mutant deficient in vFLIP IKK-γ binding, A57L-vFLIP-HA, was generated by site-directed mutagenesis using the primers K13 A57L for, 5′-CGTTTCCCCTGTT ACTAGAATGTCTGTTTCG-3′, and K13 A57L rev, 5′-CGAAACAGACATT CTAGTAACAGGGGAAACG-3′.

Production of a vFLIP-expressing lentiviral vector and transduction of HUVECs. Lentiviruses (control, vFLIP-expressing, mutant A57L-vFLIP, and HA-tagged vectors) were produced by transient cotransfection of 293T cells with the corresponding plasmids and helper plasmids (pMDLGg/p, pRSV-REV, and pMD.G, kindly provided by R. Stripecke) using the calcium phosphate transfection method. Forty-eight hours after transfection, supernatants were collected, filtered with a 0.45-μm filter, and stored at −80°C. Primary HUVECs were transduced with the lentiviral vectors in the presence of 5 μg/ml Polybrene and centrifuged at 450 × relative centrifugal force (RCF) for 30 min at 37°C. The complete medium was replaced 4 h later.

BAC mutagenesis. The KSHV-ΔFLIP construct was generated by ET cloning (Gene Bridges). The pKD46 plasmid was electroporated into DH10B-BAC36 *E. coli* and grown on Luria-Bertani (LB) agar plates under selection with chloramphenicol (15 μg/ml) and ampicillin (50 μg/ml) at 30°C. A liquid culture of *E. coli* DH10B that contains both the wild-type BAC36 and the pKD46 plasmid was induced by 0.2% L-arabinose for 1 h at 37°C to allow expression of the recombination enzymes. Approximately 0.2 μg of the *rpsL-neo* + homology cassette was then electroporated into induced (as mentioned above) and electrocompetent *E. coli* DH10B cells (2.5 kV and 25 μF in a 2-mm cuvette) and incubated for 1 h at 37°C. The resultant mutant was then selected on LB agar plates containing chloramphenicol (15 μg/ml) and kanamycin (15 μg/ml) at 37°C overnight.

The KSHV-FLIP-R construct was generated by the en passant mutagenesis strategy (65). A PCR fragment was produced using the sac isce zeo for and sac fliph zeo rev primers (see "Plasmids above") to generate a zeocin cassette flanked by a 50-bp homologous region of the vFLIP gene and SacI restriction site on one side and I-SceI and SacI restriction sites on the other side. This PCR fragment was inserted into the SacI site of vFLIP in the pEGFP-vFLIP plasmid (where EGFP is enhanced green fluorescent protein) to generate pEGFP-vFLIP-zeocin ensuring that the 50-bp vFLIP homologous region was opposite to its cognate fragment in relation to the zeocin cassette. A vFLIP-zeocin + homology cassette was generated with the VFLIP KIN FOR and VFLIP KIN REV primers using pEGFP-vFLIP-zeocin as a template. The vFLIP-zeocin + homology cassette was electroporated into GS1783-KSHV-ΔFLIP bacteria, which were preincubated at 42°C for 15 min to induce the expression of the recombining enzymes. The aim of this step is to delete the *rpsL-neo* cassette and to replace it with the vFLIP-zeocin cassette. Bacteria were plated on LB agar plates containing chloramphenicol (15 μg/ml) and zeocin (25 μg/ml) and incubated at 32°C overnight. A single bacterial colony (GS1783-KSHV-FLIP-zeo) was then grown overnight in LB medium at 32°C with chloramphenicol (15 μg/ml) and zeocin (25 μg/ml). A 100-μl aliquot was subcultured in LB medium with chloramphenicol (15 μg/ml) and grown further for 2 h. L-Arabinose (0.5%) was then added and incubated with shaking for another 30 to 60 min to induce the expression of the I-SceI enzyme. The temperature was increased to 42°C for 15 to 30 min to induce the expression of the recombining enzymes. The bacterial culture was returned to 32°C for 1 to 4 h, and then 1 μl and 0.1 μl were plated on independent LB agar plates with chloramphenicol (15 μg/ml) overnight and screened for the correct colonies by PCR the next day.

KSHV plasmid DNA was isolated from 10-ml overnight cultures by the alkaline lysis method and characterized by restriction digestion followed by Southern blotting. Large preparations KSHV DNA constructs were obtained from 500-ml *E. coli* cultures with the NucleoBond BAC 100 kit according to the manufacturer's instructions (Macherey-Nagel, Germany).

Establishment of stable KSHV-infected cell lines in HEK293, Vero, and HuAR2T-tert. To obtain HEK293 clones stably harboring the KSHV-wt, KSHV-ΔFLIP, or KSHV-FLIP-R mutants, HEK293 cells were transfected with either construct using Lipofectamine 2000 (Invitrogen) at a ratio of 1 μg DNA to 2.5 μl reagent according to the manufacturer's instructions. Twenty-four hours later, cells were trypsinized, plated in another culture plate at lower density, and grown further in DMEM supplemented with 10% FCS and penicillin-streptomycin. One day later, 150 μg/ml hygromycin B (Roche) was added to the medium, and the medium was changed every 2 to 3 days. Single clones were picked and propagated further under selection with hygromycin. The clones were called 293-KSHV-wt (for the wild type), 293-KSHV-ΔFLIP, or 293-KSHV-FLIP-R. To generate Vero producer cells, Vero cells were infected with virus produced from stable HEK293 clones and selected with hygromycin as a bulk culture. To obtain HuAR2T-tert clones stably harboring KSHV-wt, KSHV-ΔFLIP, or KSHV-FLIP-R, cells were infected with the respective virus stocks at a multiplicity of infection (MOI) of 1 and stably selected as a bulk culture.

Induction of lytic replication and detection of virus in culture supernatant. To induce lytic viral replication, KSHV-transfected or -infected cells were plated at 30 to 40% confluence. The following day, the medium was replaced with induction medium containing 1.25 mM sodium butyrate (Sigma) and Sf9 cell supernatant containing a baculovirus (a kind gift from J. Vieira) coding for KSHV RTA for 48 to 72 h. For detection and quantification of the KSHV titers, the supernatant of the induced cells was centrifuged at 5,000 × *g* for 10 min to remove floating cells. HEK293 cells (2×10^4) were plated per well of a 96-well plate and infected on the second day with a dilution of the centrifuged supernatants. Green fluorescent protein (GFP)-positive cells were counted on day 2, and the titer was calculated per ml.

To produce virus stocks for infection of HUVECs, a large-scale virus production was prepared in 175-cm^2 flasks and induced to 30 to 40% confluence as described above. The supernatant was harvested 48 to 72 h later and centrifuged at 5,000 × *g* for 10 min. The cleared supernatant was collected in centrifuge bottles (230 ml/bottle) and centrifuged at 18,000 rpm for 4 h using a type 19 rotor in a Beckman ultracentrifuge. The supernatant was then discarded, and the pellet was resuspended in 300 μl medium overnight at 4°C. The resuspended virus was kept at 4°C.

Southern blot analysis. Purified KSHV-wt or mutant DNA was digested with NruI and separated on 0.4% agarose gels in 0.5× Tris-borate-EDTA (TBE) buffer for 14 to 18 h at 2.5 V/cm. DNA fragments were visualized by ethidium bromide staining, denatured with NaOH, and transferred to a Hybond-N+ membrane (Amersham). DNA probes were labeled with alkaline phosphatase by AlkPhos Direct labeling and detection system (Amersham). Blocking was performed at 65°C for 15 min in hybridization buffer. DNA blots were hybridized with labeled probes in the same buffer at 65°C for about 16 h. Blots were washed twice for 10 min in primary wash buffer at 65°C and twice for 5 min with the secondary wash buffer at room temperature. Detection of the hybridized probes was performed by chemiluminescence with CDP-Star (Amersham).

Northern blot analysis. Total RNA was harvested using RNA-Bee (AMS Biotechnology, Abingdon, United Kingdom) according to the manufacturer's instructions and analyzed by Northern blotting as described previously (59). Briefly, 14 μg of total RNA was electrophoresed through 15% acrylamide urea denaturing gels and transferred by electroblotting to Zeta-Probe GT membranes (Bio-Rad, Hercules, CA). Antisense oligonucleotide probes specific for KSHV microRNAs (miRNAs) were radiolabeled using T4 polynucleotide kinase (NEB, Ipswich, MA) and hybridized in ExpressHyb hybridization buffer (BD Biosciences Clontech, Mountain View, CA) according to the manufacturer's instructions. The blots were subsequently subjected to autoradiography.

Immunoblotting. Cell lysates were separated on SDS-PAGE gels and transferred onto nitrocellulose membranes (Amersham) using a Mini Trans-Blot unit (Bio-Rad) for 60 min at 350 mA. The membranes were blocked for 1 h in Tris-buffered saline containing 0.1% Tween 20 and 5% Marvel (TBST-M) and incubated overnight at 4°C with the primary antibody diluted in TBST-M. After a washing step, the membranes were incubated for 1 h with a peroxidase-conjugated secondary antibody diluted in TBST-M. Following further washing steps, the proteins were detected with a chemiluminescence kit (PerkinElmer Life Sciences).

Gene expression microarray experiments. Total RNA was extracted with the RNeasy microkit (Qiagen) according to the manufacturer's recommendation and was subjected to a whole-human-genome microarray analysis (G4112F, AMADID 014850; Agilent Technologies) that covers the entire human transcriptome. Syn-

thesis of cRNA was performed with the one-color Quick Amp labeling kit (Agilent Technologies) according to the manufacturer's recommendation. cRNA fragmentation, hybridization, and washing steps were performed exactly as recommended by the manufacturer of One-Color Microarray-Based Gene Expression Analysis, version 5.7 (Agilent), except that 2.5 μg of each labeled cRNA sample was used for hybridization. Slides were scanned on an Agilent microarray scanner, model G2505 B, at two different photomultiplier tube (PMT) settings (100% and 5%) to increase the dynamic range of the measurements. Data extraction was performed with the Feature Extraction software, version 9.5.3.1, by using the recommended default extraction protocol file: GE1-v5_95_Feb07.xml.

Processed intensity values of the green channel (gProcessedSignal or gPS) were globally normalized by linear scaling: all gPS values of one sample were multiplied by an array-specific scaling factor. This factor was calculated by dividing the 75th-percentile value taken from one selected reference array, contained within the series, by the 75th-percentile value of the particular microarray ("array *i*" in the formula shown below). Accordingly, normalized gPS values for all samples (microarray data sets) were calculated by the following formula: normalized gPS array i = gPS array $i \times$ (75th-percentile reference array/75th percentile array i). An appropriate low-intensity threshold was established, based primarily on (i) the intensity distribution at the low-intensity end and (ii) the attribute "*g* is well above BG" (determined by the Feature Extraction software; *g* is green processed signal, and BG is background). The established threshold values were 34 (vFLIP overexpression experiments) and 120 (KSHV infection experiments). All of those normalized gPS values that fell below this intensity border were replaced by corresponding surrogate values of 34 and 120, respectively.

qPCR analysis. Total RNA, used in the microarray experiments, was reverse transcribed using 50 U of BioScript low-RNase H reverse transcriptase (BIO-27036; Bioline) in 20-μl reaction mixtures. The enzyme was finally inactivated for 10 min at 70°C. Aliquots of generated cDNA samples were used for quantitative PCR (qPCR) with the ABI 7500 Fast qPCR system (Applied Biosystems). Specific amplification was ensured by using TaqMan probes and gene-specific primers. Amplification was performed in 10-μl reaction mixtures by use of TaqMan universal PCR master mix under recommended conditions (catalog no. 4364341; Applied Biosystems).

The following primers, probes, and assays were used: EGFP forward primer GTCCGCCCTGAGCAAAGA, EGFP reverse primer TCCAGCAGGACCAT GTGATC, EGFP probe FAM-CCCAACGAGAAGCG-MGBNFQ, where FAM is 6-carboxyfluorescein, K8 forward primer AATTCCACATCCCCGATC CTTC, K8 reverse primer CTTAGTGCATAAGCGTTCCTCTTC, and K8 probe FAM-CACACACCACCAAGAGGACCACACA-TAMRA, where TAMRA is tetramethylrhodamine. The average cycle threshold (C_T) value for each individual amplification reaction was calculated from duplicate or triplicate measurements by means of the instrument's software in auto-C_T mode (7500 Fast system software, version 1.3.0). Average C_T values calculated for EGFP or K8 were normalized by subtraction from the C_T values obtained for GAPDH (glyceraldehyde-3-phosphate dehydrogenase).

Reverse transcriptase PCR. Total RNA was extracted from the cells with an RNeasy kit (Qiagen) according to the manufacturer's instructions, followed by DNA-free DNase treatment and inactivation according to the manufacturer's instructions (Ambion). cDNA was synthesized using the Expand reverse transcriptase (Roche) and oligo(dT) primer at 42°C for 1 h. Conventional PCR was then performed to amplify vFLIP, vCyc, and GAPDH transcripts using the following primers, respectively: K13 seq for (5′-TACAGTACACCCAGTGTA AG-3′), K13 seq rev (5′-TTACGAGGTTCTCTGTGAGG-3′), vCYC seq 4 for (5′-CATCGCATCCCAATATGCTTGC-3′), vCYC seq 5 rev (5′-ACGCTATG TGAGGATCGGATC-3′), GPDH3 (5′-TCCACCACCCTGTTGCTGTA-3′), and GPDH5 (5′-ACCACAGTCCATGCCATCAC-3′).

Immunofluorescence assay. Vero cells infected with KSHV-wt, KSHV-ΔFLIP, or KSHV-FLIP-R and selected with hygromycin were plated on glass coverslips in 6-well plates. Twenty-four hours later, cells were fixed with 4% paraformaldehyde in phosphate-buffered saline (PBS) for 20 min and then neutralized with 10% NH_4Cl for 10 min. The fixed cells were permeabilized with 0.2% Triton X-100 in PBS for 10 min. Cells were rinsed with PBS, incubated with 10% FCS in PBS for 20 min, and then rinsed again with PBS. Coverslips were incubated for 1 h at 37°C in a humidified chamber with the primary antibody in PBS containing 1% bovine serum albumin (BSA). Coverslips were washed in PBS three times and incubated with the secondary antibody plus DAPI (4′,6-diamidino-2-phenylindole) in 1% BSA in PBS and then rinsed with PBS.

RESULTS

Construction and verification of KSHV-ΔFLIP and KSHV-FLIP-R. To study the role of vFLIP in the context of the viral genome, we took advantage of having the KSHV genome cloned as a bacterial artificial chromosome (BAC) (73). KSHV-ΔFLIP was generated using the ET cloning technique. A cassette encoding kanamycin resistance (*rpsL-neo* cassette) flanked by 60-bp sequences bordering the region to be deleted was electroporated into the *E. coli* strain DH10B harboring the KSHV-wt and the pKD46 plasmid, which encodes the recombination enzymes under the control of an L-arabinose-inducible promoter (Fig. 1A). KSHV-ΔFLIP, as a result of the cassette insertion, lacks the whole vFLIP gene, corresponding to nucleotide position 122959, upstream of the vFLIP start codon, and nucleotide position 122393, downstream of the stop codon (GenBank accession no. AF148805) (Fig. 1A).

vFLIP was reinserted in its original position to generate the KSHV-FLIP-R construct using a two-step markerless mutagenesis strategy termed "en passant mutagenesis" (65). The *rpsL-neo* cassette in the KSHV-ΔFLIP construct was replaced by a vFLIP-zeocin + homology cassette using an ET cloning strategy. This cassette contains the vFLIP gene with a zeocin resistance-coding DNA sequence inserted in its SacI site and a 50-bp fragment of vFLIP (indicated by black boxes in Fig. 1B) duplicated on both sides of the zeocin gene to create homology for the next step. On the left side of the zeocin gene, an I-SceI restriction site had previously been inserted (Fig. 1B). In the next step, the expression of the I-SceI enzyme was induced by 1% arabinose to cut the unique site between zeocin and the duplicated fragment of vFLIP. Directly afterward, the expression of the recombination enzymes was induced at 42°C to initiate the homologous recombination of the duplicated vFLIP region (Fig. 1B).

After a screening for positive colonies by PCR (data not shown), the DNA of KSHV-wt, KSHV-ΔFLIP, and KSHV-FLIP-R were digested with NruI. The insertion of the *rpsL-neo* cassette replaced the 566-bp vFLIP fragment with a 1,320-bp fragment, leading to a shift of the 14-kb band in KSHV-ΔFLIP by 754 bp (indicated by the arrow in Fig. 1C). The reinsertion of vFLIP shifted this band to its position in the KSHV-wt genome. For further verification, the three constructs were also digested with several other restriction enzymes (KpnI, EcoRI, SacI [data not shown]). To confirm the specificity of the band shift in the NruI digestion pattern and to exclude the possibility that the *rpsL-neo* cassette was inserted twice in the genome, the gel was analyzed by Southern blotting. The digested DNA was transferred to a nylon membrane and hybridized with the *rpsL-neo* probe labeled with alkaline phosphatase, which showed the presence of one specific band only in KSHV-ΔFLIP (Fig. 1C, lanes 5, 6, and 7). The membrane was stripped and rehybridized with a vFLIP PCR fragment labeled with alkaline phosphatase. One specific band was detected in KSHV-wt and KSHV-FLIP-R but not in KSHV-ΔFLIP (Fig. 1C, lanes 8, 9, and 10). The junction regions, as well as the newly inserted vFLIP gene, were also sequenced and proved to be identical to the wt sequence (data not shown).

Deletion of vFLIP does not affect the expression of neighboring viral genes. vFLIP is located in the KSHV genome between LANA and vCyc (upstream) and a cluster of miRNAs

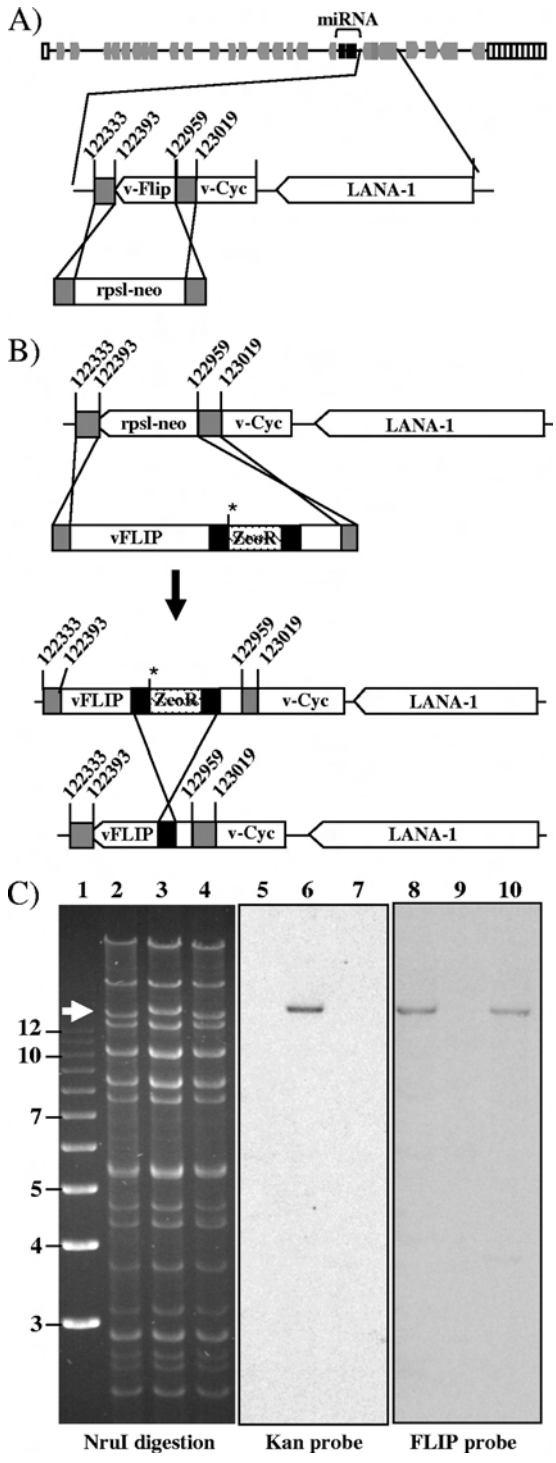

FIG. 1. Construction of the KSHV-ΔFLIP and KSHV-FLIP-R genomes. (A) A kanamycin resistance cassette flanked by 60-bp homologous regions surrounding the vFLIP (shown in gray) was inserted by homologous recombination in the indicated area, resulting in a complete vFLIP gene knockout. Numbers are according to the sequence of GenBank accession no. AF148805. (B) A zeocin resistance cassette was inserted into the SacI site in vFLIP and flanked by a duplicated region of vFLIP (shown in black) in addition to a unique I-SceI restriction site (indicated by an asterisk). The whole cassette was also flanked by 50-bp homologous regions (in gray) surrounding the kanamycin resistance cassette in KSHV-ΔFLIP. This cassette, instead of the kanamycin cassette, was inserted by homologous recombination, placing vFLIP back in its authentic position in the KSHV genome. In a second step, I-SceI was used to cut in its unique site, allowing homologous recombination of the duplicated vFLIP sequences on either side of the Zeo^r cassette and thus combination of the two parts of vFLIP without extra DNA in the genome. (C) NruI digestion and Southern blotting of KSHV-wt, KSHV-ΔFLIP, and KSHV-FLIP-R. The KSHV genomic DNA was isolated from 10 ml overnight bacterial cultures of the constructs using the alkaline lysis and alcohol precipitation method. The DNA was digested with NruI enzyme for 4 h, loaded onto 0.4% agarose, and allowed to run overnight. Lane 1 contains a 1-kb marker. Lanes 2, 5, and 8 represent KSHV-wt; lanes 3, 6, and 9 represent KSHV-ΔFLIP; and lanes 4, 7, and 10 represent KSHV-FLIP-R. The arrow shows the expected band shift due to the replacement of vFLIP with the *rpsL-neo* cassette. For Southern blotting, the DNA was transferred onto a nylon membrane and hybridized with the alkaline phosphatase-labeled *rpsL-neo* probe and then stripped and rehybridized with the vFLIP probe.

(downstream) (Fig. 1A). We checked the expression of these genes to ensure the integrity of our KSHV constructs. Total RNA was extracted from HEK293 cell lines stably transfected with KSHV-wt, KSHV-ΔFLIP, or KSHV-FLIP-R and treated with DNase I. The cDNA was prepared using the oligo(dT) primer. Specific primers were then used to amplify the vFLIP, vCyc, and GAPDH genes (see Materials and Methods). The vCyc transcript was present in all clones, while vFLIP was absent in the KSHV-ΔFLIP clone only (Fig. 2A). Empty HEK293 cells showed neither vCyc nor vFLIP bands indicating the specificities of the primers. The same RT-PCR without reverse transcriptase showed no signal for any of the tested genes, excluding the possibility of genomic DNA amplification (data not shown). LANA expression was tested by immunofluorescence assay (IFA) on Vero cell lines stably harboring the KSHV-wt, KSHV-ΔFLIP, or KSHV-FLIP-R genome. All clones showed the presence of the characteristic LANA speckles in the nucleus (Fig. 2B). The miRNAs are located downstream of vFLIP and are transcribed from the same promoter with vCyc and vFLIP. Nonetheless, deletion of vFLIP did not affect the expression of these miRNAs, as shown by the transcription of the miRNA K12-10 (Fig. 2C).

Contribution of KSHV vFLIP to spindle cell formation in infected primary endothelial cells. Spindle cells are the hallmark of KS lesions and considered to be tumor cells. *In vitro*, KSHV has been shown to infect lineages of endothelial cells, including those of lymphatic and microvascular origins, and to induce spindling reminiscent of that in KS lesions (10, 18, 24, 26, 32, 67). Overexpression of vFLIP in endothelial cells using retroviral or lentiviral vectors has been shown to induce spindling in an NF-κB-dependent manner (21, 29, 42).

To investigate the contribution of vFLIP to KSHV-induced spindle cell formation in the context of the whole virus, a monolayer of primary human umbilical vein endothelial cells (HUVECs) was infected with KSHV-wt, KSHV-ΔFLIP, or KSHV-FLIP-R at a multiplicity of infection (MOI) of approximately 0.2 for HUVECs. KSHV-wt, KSHV-ΔFLIP, and KSHV-FLIP-R stocks were produced in stably infected Vero cells, as described in Materials and Methods. GFP expression, encoded by the recombinant virus (BAC36-KSHV), was used to monitor the infected endothelial cells. Green cells were observed at 1 day postinfection in all infected culture plates.

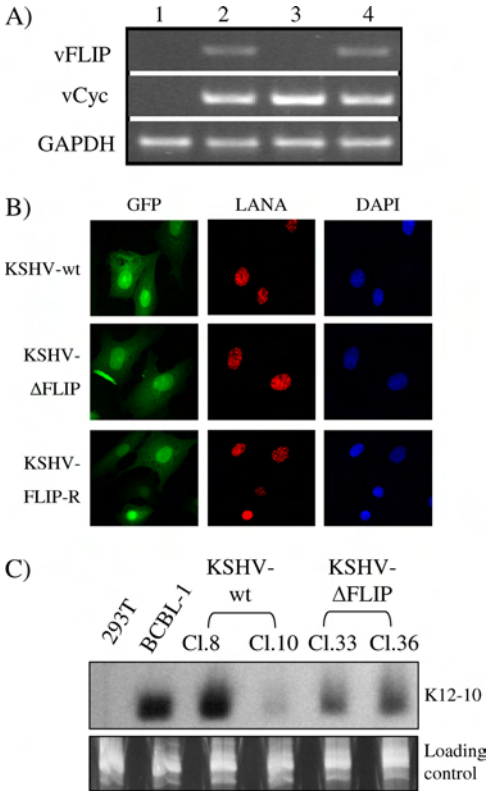

FIG. 2. Deletion of vFLIP does not affect the expression of flanking genes. (A) Results of RT-PCR of total RNA extracted from the HEK293 cell line stably maintaining the indicated KSHV constructs showing the presence of vFLIP and vCyc transcripts in KSHV-wt and vFLIP-R constructs and the absence of the vFLIP transcript in the case of the KSHV-ΔFLIP clone. Lane 1, HEK293 cells; lane 2, HEK293 KSHV-wt clone; lane 3, HEK293 KSHV-ΔFLIP clone; and lane 4, HEK293 KSHV-FLIP-R clone. (B) IFA showing the expression of LANA in Vero cells stably infected with KSHV-wt, KSHV-ΔFLIP, or KSHV-FLIP-R. (C) Northern blot analysis showing the transcription of the K12-10 miRNA in HEK293 cell lines stably transfected with the KSHV-wt or KSHV-ΔFLIP genome (two different cell lines were tested for each virus).

Cells infected with the wild-type virus or the vFLIP revertant virus showed spindling morphology, in contrast to the cells infected with the vFLIP knockout virus (Fig. 3A), in line with the effects of overexpressed vFLIP on endothelial spindle cell formation (21, 29, 42). However, at a higher MOI (MOI of approximately 1 for HUVECs), HUVECs infected with KSHV-ΔFLIP also showed spindling morphology similar to that in KSHV-wt- or KSHV-FLIP-R-infected cells (Fig. 3B).

vFLIP enhances the survival of KSHV-infected cells. During our experiments, we observed a more rapid loss of KSHV-ΔFLIP-infected HUVECs from culture plates than that of KSHV-wt- or KSHV-FLIP-R-infected cells, indicating a role for vFLIP in the maintenance or survival of infected cells. To quantify the effect of vFLIP on the persistence of KSHV-infected cells, HUVECs were plated in 24-well plates and infected at an MOI for HUVECs of approximately 0.1 with KSHV-wt, KSHV-ΔFLIP, or KSHV-FLIP-R. Infected cells, monitored by GFP expression, were counted every 2 days, and the results are expressed as percentages of the counts at the first time point, 2 days after infection. The number of

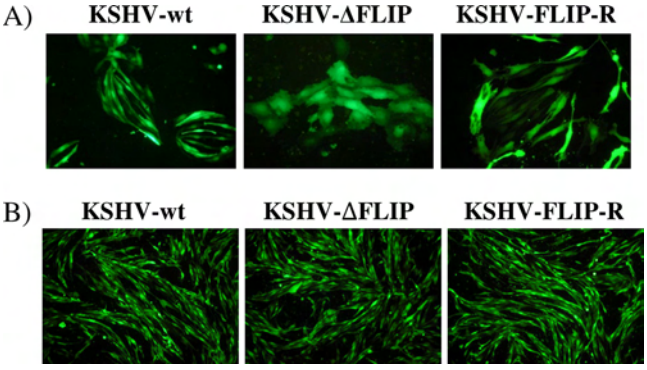

FIG. 3. vFLIP contributes to spindle cell formation of KSHV-infected HUVECs. (A) A monolayer of HUVECs was infected with the indicated KSHV-wt, KSHV-ΔFLIP, or KSHV-FLIP-R at an MOI of 0.2 for HUVECs and monitored for up to 2 weeks. Images were taken 10 days after infection. (B) A monolayer of HUVECs was infected with the indicated KSHV variants at an MOI of 1 for HUVECs. Images were taken 5 days after infection.

HUVECs infected with all three KSHV variants increased during the first 4 days after infection, suggesting replication of infected cells at early stages of infection (Fig. 4). KSHV-ΔFLIP-infected HUVECs showed the smallest increase by day 4, and their number decreased faster than in KSHV-wt- or FLIP-R-infected cells (Fig. 4). There was a significant difference between the percentages of KSHV-wt- and KSHV-ΔFLIP-infected cells, as well as of KSHV-FLIP-R- and KSHV-ΔFLIP-infected cells (data not shown). This result suggests that vFLIP provides a moderate growth advantage to KSHV-infected endothelial cells.

Differential gene expression analysis of KSHV-wt- or KSHV-ΔFLIP-infected HUVECs. To further understand the contribution of vFLIP to KSHV pathogenesis and oncogenesis, we compared the whole transcriptome pattern from KSHV-wt- and KSHV-ΔFLIP-infected HUVECs on a whole-human-genome microarray. HUVECs were plated in 24-well plates and infected the next day at an MOI of approximately 1 with KSHV-wt, KSHV-ΔFLIP, or heat-inactivated KSHV-wt. Four days after infection, cells were lysed, and total RNA was ex-

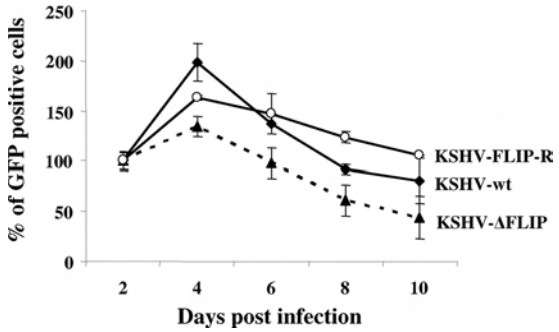

FIG. 4. vFLIP contributes to the maintenance of KSHV-infected cells. HUVECs were plated in 24-well plates and infected the next day with the KSHV-wt, KSHV-ΔFLIP, or KSHV-FLIP-R construct at an MOI of 0.1. GFP-positive cells were counted at the indicated time points, and the percentage of GFP-positive cells relative to the count at the first time point was calculated. Each time point represents the average of counts from three different wells.

tracted and processed using Agilent standard protocols and hybridized onto whole-genome 4X44K microarrays. Two independent experiments were performed on cells from two different donors using different virus preparations. The level of GFP mRNA in KSHV-ΔFLIP-infected cells was comparable to that in KSHV-wt-infected cells, indicating comparable rates of infection (data not shown).

We compared the cellular gene expression profiles from our microarray experiments (KSHV-wt versus KSHV-ΔFLIP infection) to the expression profile obtained from HUVECs transduced for 72 h with a lentiviral vector for vFLIP (see Materials and Methods) and to those of two other previously published whole-genome microarray studies employing overexpression of vFLIP via a retrovirus (53, 64). In agreement with the two previously published studies, vFLIP overexpression in HUVECs showed a consistent upregulation of a large set of genes (Fig. 5A and B, columns 1 and 2). Among the vFLIP-induced genes were those for several cytokines and their receptors (e.g., IL-1β, IL-7 receptor [IL-7R], and IL-18R), genes for chemokines (IL-8, CXCL10, CCL5, CXCL5, CXCL6, and CCL20), genes involved in antiapoptotic processes (BCL2A1, BIRC3, XAF1, and SOD2 genes), genes with proapoptotic functions (RIPK2 and TNFRSF19 genes), and many antiviral and interferon (IFN)-inducible genes (MX1 and -2, OAS-1-3, viperin, and IFI6 genes). Interestingly, the expression of only a few of the genes induced by overexpressed vFLIP turned out to be significantly upregulated in KSHV-infected HUVECs compared to their expression in ΔFLIP-infected cells (Fig. 5A and B). Only a group of 15 cellular genes that were induced more than 2-fold by vFLIP overexpression in this study and in the studies by Sakakibara et al. (53) and Thurau et al. (64) were also upregulated in KSHV-wt-infected cells, in comparison to KSHV-ΔFLIP-infected cells (Fig. 6). The expression of these 15 differentially regulated genes was also increased in HUVECs treated with either alpha or beta interferon (results not shown; see the summary in Fig. 6), suggesting that, in the context of the viral genome and during viral latency, vFLIP shows the strongest effect on a set of interferon-regulated cellular genes. However, overexpression of vFLIP did not upregulate the expression of type I or type II interferon genes (data not shown), suggesting that the upregulation of interferon-responsive genes in KSHV-wt- versus KSHV-ΔvFLIP-infected cells is not due to an increased expression of type I or II interferons.

vFLIP induces STAT1 and STAT2 phosphorylation. As vFLIP induced the expression of interferon-responsive genes without inducing type I or II interferon genes, we investigated the impact of vFLIP on the signaling cascade downstream of the interferon receptor. We transduced HUVECs with a lentivirus expressing either vFLIP or an IKK-γ-binding-deficient mutant (vFLIP-A57L) in the form of GFP–T2A–vFLIP-wt–HA, GFP-T2A-vFLIP-A57L, or the control lentivirus. vFLIP-HA and the IKK-γ-binding-deficient mutant are cleaved cotranslationally into a GFP-T2A fusion protein and vFLIP-HA. Cells were lysed 48 h after transduction and tested for JAK1, JAK2, Tyk2, and STAT1 to STAT6 expression and phosphorylation by immunoblotting. vFLIP induced the phosphorylation of STAT1 on both residues tyrosine 701 and serine 727, along with a moderate increase in the STAT1 protein level (Fig. 7A). Additionally, vFLIP induced the upregulation and phosphorylation of STAT2 on the tyrosine 690 residue (Fig. 7A) but not STAT3, STAT5, or STAT6 (Fig. 7A, C, and D). vFLIP also upregulated the expression of JAK2 and slightly that of JAK1 and Tyk2 without inducing an increase in their phosphorylation (Fig. 7B). This upregulation of JAK2/STAT1/STAT2 and the increased phosphorylation of STAT1 and STAT2 are NF-κB dependent because the vFLIP-A57L mutant, which is completely defective in NF-κB activation (2), failed to induce STAT1 and STAT2 phosphorylation (Fig. 7A and B). Furthermore, knockdown of either IKK-γ or RelA (p65) by siRNA prevents vFLIP-mediated STAT1 and STAT2 phosphorylation (Fig. 7E). Knocking down JAK2 expression by siRNA had only a moderate effect on vFLIP-mediated STAT1/STAT2 phosphorylation (Fig. 7E), while knocking down either JAK1 or Tyk2 had no appreciable effect on vFLIP-mediated STAT1/STAT2 phosphorylation (Fig. 7F).

Furthermore, vFLIP seems to phosphorylate STAT1 and STAT2 in a cell type-dependent manner. While vFLIP induces the upregulation and phosphorylation of STAT1 at both the tyrosine 701 and serine 727 residues and STAT2 in primary endothelial cells as well as in HeLa cells (Fig. 7A and 8), it does not have this effect in B cells like BJAB or KSHV-infected primary effusion lymphoma cells (BCBL-1) (Fig. 8). vFLIP also fails to activate or phosphorylate STAT1 and STAT2 in other epithelial cell lines like Vero and HEK293 cells (data not shown).

Furthermore, to determine the role of vFLIP-mediated STAT1 and STAT2 phosphorylation in the context of the entire virus, we analyzed the phosphorylation levels of STAT1/STAT2 in KSHV-wt-, KSHV-ΔFLIP-, and KSHV-FLIP-R-infected, conditionally immortalized endothelial cell lines (HuAR2T-tert) (Fig. 9). HuAR2T-tert cells were infected with KSHV-wt, KSHV-ΔFLIP, or KSHV-FLIP-R at an MOI of 1 and selected with hygromycin to generate stable cell lines. All hygromycin-selected lines showed close to 100% GFP expression (data not shown). Stably selected cells were plated in 6-well plates and were lysed 24 h later. The cellular lysates were analyzed for STAT1/STAT2 phosphorylation. KSHV-ΔFLIP-infected cells showed a reduction in the levels of phosphorylated STAT1/STAT2 relative to those in KSHV-wt- and KSHV-FLIP-R-infected cells. As expected, the induction of STAT1/STAT2 phosphorylation in KSHV-wt- and KSHV-vFLIP-R-infected cells was less pronounced than in endothelial cells in which vFLIP had been overexpressed by means of a lentiviral vector (Fig. 9). Taken together, our data suggest that vFLIP induces the phosphorylation of STAT1/STAT2 in endothelial cells in the context of the entire virus.

The complete transcriptome profile of KSHV-infected HUVECs or vFLIP-transduced HUVECs is available upon request (contact Oliver Dittrich-Breiholz at dittrich.oliver@mh-hannover.de).

DISCUSSION

The aim of this study was to investigate the role of vFLIP in the context of the entire viral genome during viral persistence in endothelial cells and to assess the contribution of vFLIP-induced effects previously found in studies that overexpressed vFLIP in endothelial cells. As it is translated from the second exon of a bicistronic mRNA by means of an internal ribosome

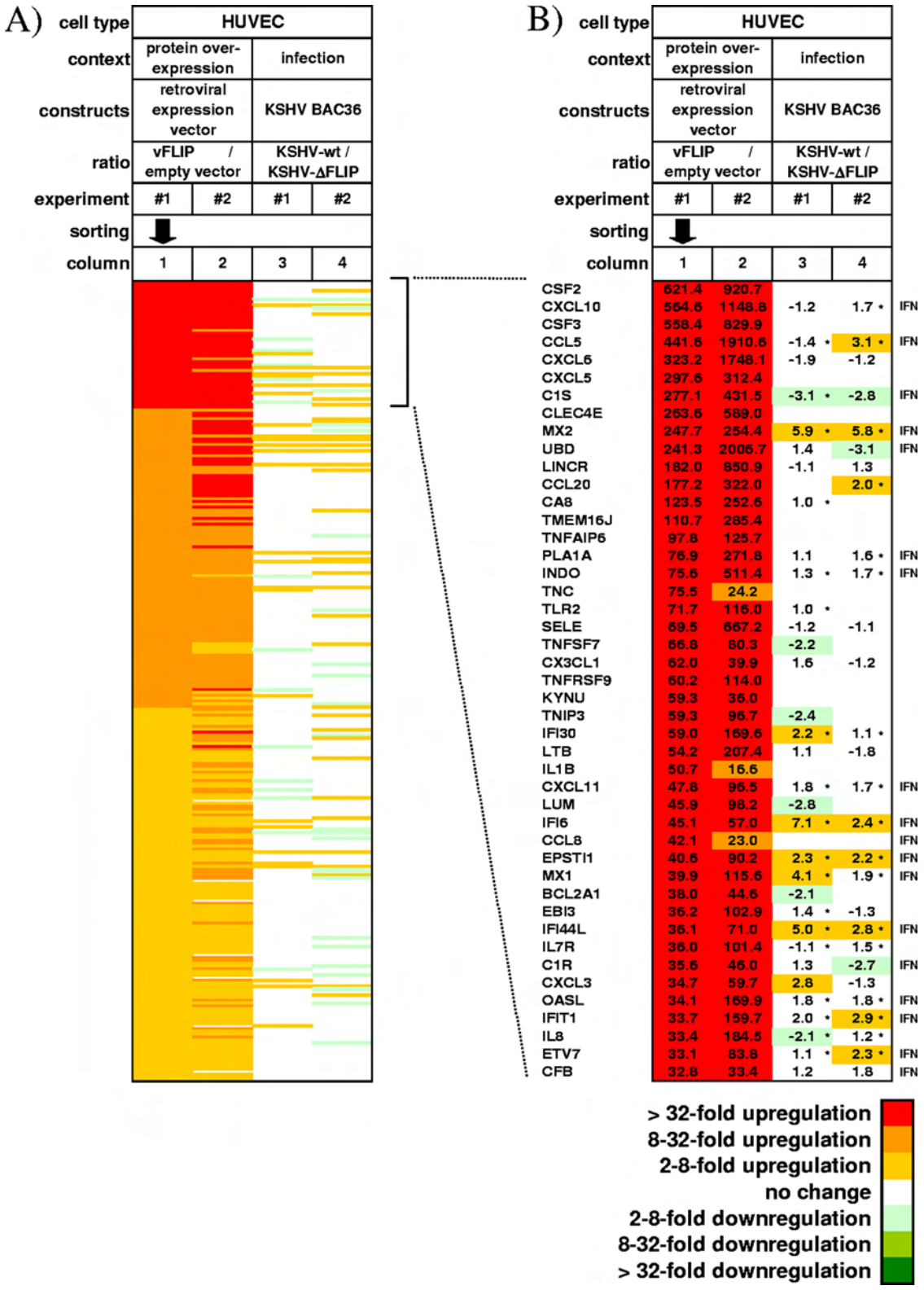

FIG. 5. Only a subset of cellular genes consistently upregulated by overexpressed vFLIP are differentially expressed in KSHV-wt- and KSHV-ΔvFLIP-infected cells. (A) Microarray analysis of HUVECs infected at an MOI of approximately 1 with either KSHV-wt or KSHV-ΔFLIP, compared to HUVECs transduced with the vFLIP-expressing vector. Filters were set to exclude all flagged values and poorly annotated or poorly characterized transcripts. Depicted are 281 genes, which showed more than 4-fold upregulation in vFLIP-transduced cells compared to their expression levels in control-vector-transduced cells in one (experiment 1, column 1) out of two experiments performed (columns 1 and 2). Columns 3 and 4 represent the differential regulation of these genes in HUVECs infected with KSHV-wt or KSHV-ΔFLIP in two independent experiments. Ratio values were calculated from processed signal intensities of KSHV-wt-infected/KSHV-ΔFLIP-infected HUVEC samples and are color coded

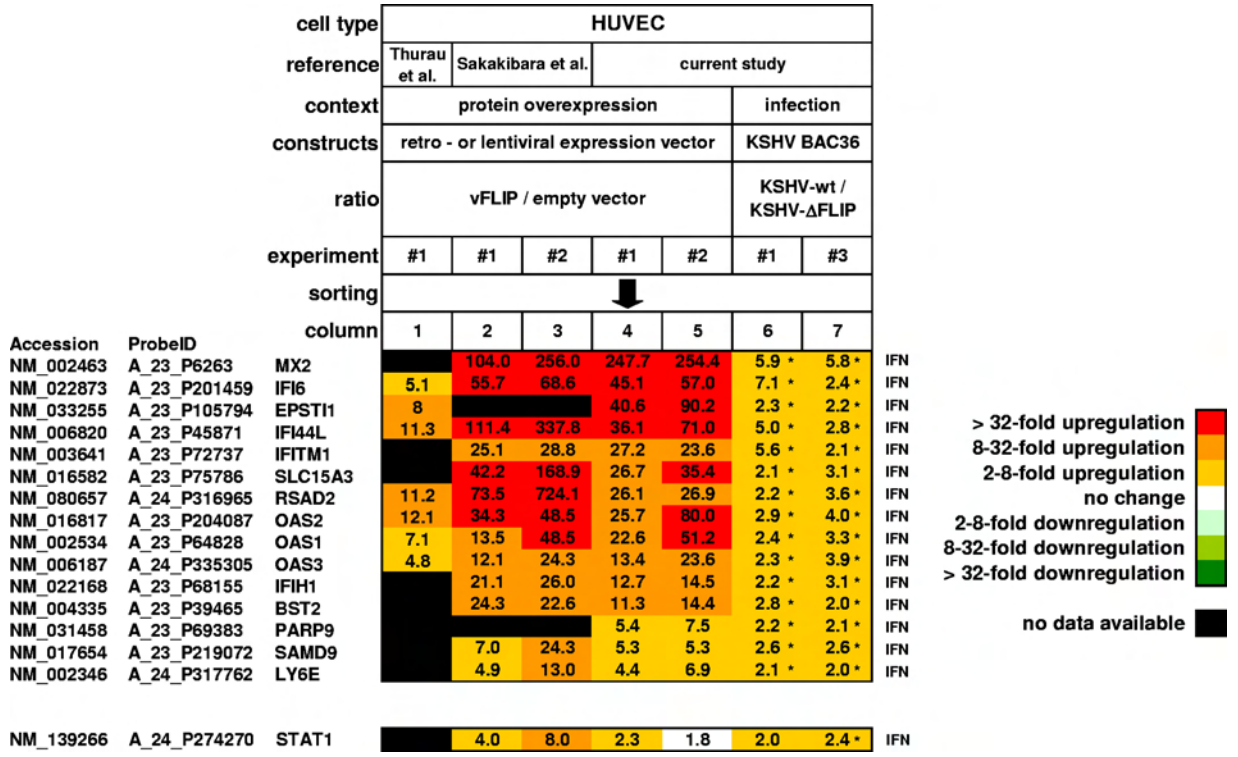

FIG. 6. Genes from Fig. 5A, which were induced at least 2-fold by transduced vFLIP in three studies (see below) and which were also upregulated at least 2-fold in KSHV-wt- versus KSHV-ΔvFLIP-infected HUVECs. Lane 1, response to retrovirally transduced vFLIP as reported by Thurau et al. (64); lanes 2 and 3, response to transduced vFLIP as reported by Sakakibara et al. (53); lanes 4 and 5, response to lentivirally transduced vFLIP (this study); lanes 6 and 7, cellular genes upregulated at least 2-fold in KSHV-wt- versus KSHV-ΔvFLIP-infected HUVECs in two independent experiments. Asterisks indicate genes that were induced more than 2-fold in KSHV-wt-infected cells compared to in cells infected with heat-inactivated KSHV. The designation "IFN" to the right of the table indicates that this gene was responsive to IFN-α and IFN-β in an experiment conducted on primary endothelial cells (our unpublished results).

entry site (IRES) (6, 38), vFLIP protein levels in PEL cells or infected endothelial cells are low (38) (Fig. 9 and data not shown), and effects ascribed to vFLIP on the basis of its overexpression in transfected or transduced cells may therefore be mitigated in the context of the natural infection.

Among these effects is the ability of vFLIP to induce endothelial cell spindling when transduced into primary endothelial cells (21, 29, 42, 53, 64). We found that a vFLIP knockout virus was not able to induce spindling morphology in HUVECs infected at a low MOI, suggesting a role for vFLIP in KSHV-infected cell morphogenesis. However, other viral proteins may contribute to the spindle cell phenotype, since we did observe spindle cell formation in HUVEC infection with KSHV-ΔFLIP at an MOI of approximately 1. Grossmann et al. and others showed that the inhibition of NF-κB activation prevents vFLIP-induced spindling in HUVECs (21, 29, 42, 53) and that the equine herpesvirus 2 vFLIP, which does not activate NF-κB, could not induce spindle cell formation, suggesting a link between NF-κB formation and KSHV vFLIP-induced spindling (29). It is thus possible that other NF-κB-activating viral genes could contribute to spindle cell formation, like *K1*, *K15*, *orf75*, or *mirK1* (8, 36, 37, 54, 68). There is evidence for the expression of all of these genes, with the exception of *orf75*, in latently/persistently infected cells (9, 13, 30, 51, 55). However, since infection at a low MOI probably reflects the *in vivo* situation more closely, vFLIP is likely to be an important player in KSHV-induced spindle cell formation.

As an oncogenic virus, KSHV provides infected cells with a survival advantage (69). We observed that endothelial cells infected with KSHV-wt have a moderate growth advantage over KSHV-ΔFLIP-infected cells. This function of vFLIP was previously reported also in PEL cells (27, 31). Thus, vFLIP plays a vital role in KSHV pathogenesis in infected endothelial cells as well as B cells by enhancing their survival most likely via NF-κB activation.

Several groups have shown that the ectopic expression of vFLIP in HUVECs leads to the upregulation of hundreds of genes with diverse functions (52, 53, 64), and we could confirm

appropriately. (B) Selective representation of the 45 genes upregulated by vFLIP more than 32-fold. Asterisks indicate genes that were induced more than 2-fold in KSHV-wt-infected cells compared to cells mock infected with heat-inactivated virus. The designation "IFN" to the right of the table indicates that this gene was responsive to IFN-α and IFN-β in an experiment conducted on primary endothelial cells (our unpublished results). Empty cells in the column correspond to an undetectable mRNA level.

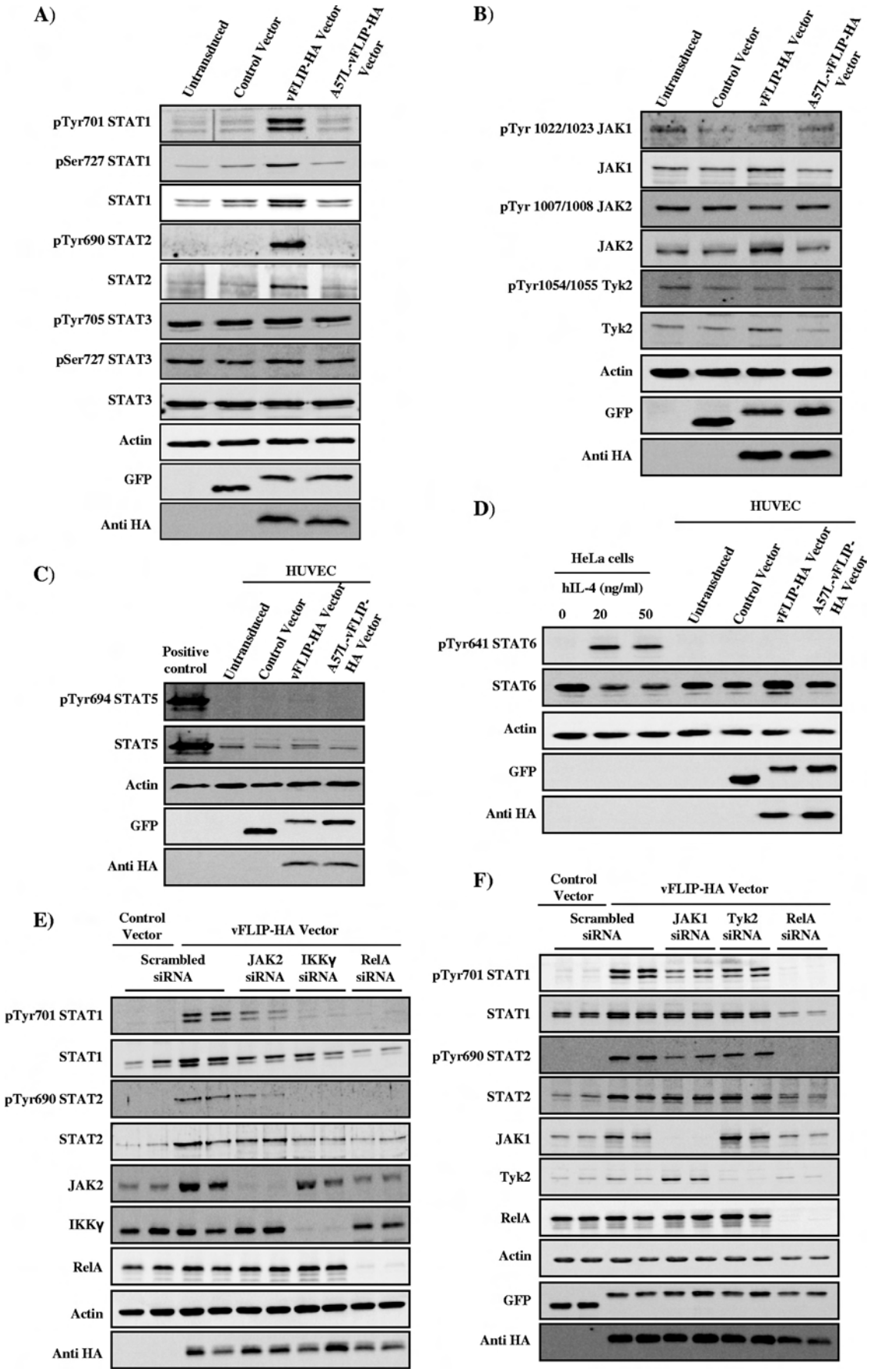
A)
Untransduced
Control Vector
vFLIP-HA Vector
A57L-vFLIP-HA Vector
pTyr701 STAT1
pSer727 STAT1
STAT1
pTyr690 STAT2
STAT2
pTyr705 STAT3
pSer727 STAT3
STAT3
Actin
GFP
Anti HA
B)
Untransduced
Control Vector
vFLIP-HA Vector
A57L-vFLIP-HA Vector
pTyr 1022/1023 JAK1
JAK1
pTyr 1007/1008 JAK2
JAK2
pTyr1054/1055 Tyk2
Tyk2
Actin
GFP
Anti HA
C)
HUVEC
Positive control
Untransduced
Control Vector
vFLIP-HA Vector
A57L-vFLIP-HA Vector
pTyr694 STAT5
STAT5
Actin
GFP
Anti HA
D)
HUVEC
HeLa cells
hIL-4 (ng/ml)
0
20
50
Untransduced
Control Vector
vFLIP-HA Vector
A57L-vFLIP-HA Vector
pTyr641 STAT6
STAT6
Actin
GFP
Anti HA
E)
Control Vector
vFLIP-HA Vector
Scrambled siRNA
JAK2 siRNA
IKKγ siRNA
RelA siRNA
pTyr701 STAT1
STAT1
pTyr690 STAT2
STAT2
JAK2
IKKγ
RelA
Actin
Anti HA
F)
Control Vector
vFLIP-HA Vector
Scrambled siRNA
JAK1 siRNA
Tyk2 siRNA
RelA siRNA
pTyr701 STAT1
STAT1
pTyr690 STAT2
STAT2
JAK1
Tyk2
RelA
Actin
GFP
Anti HA

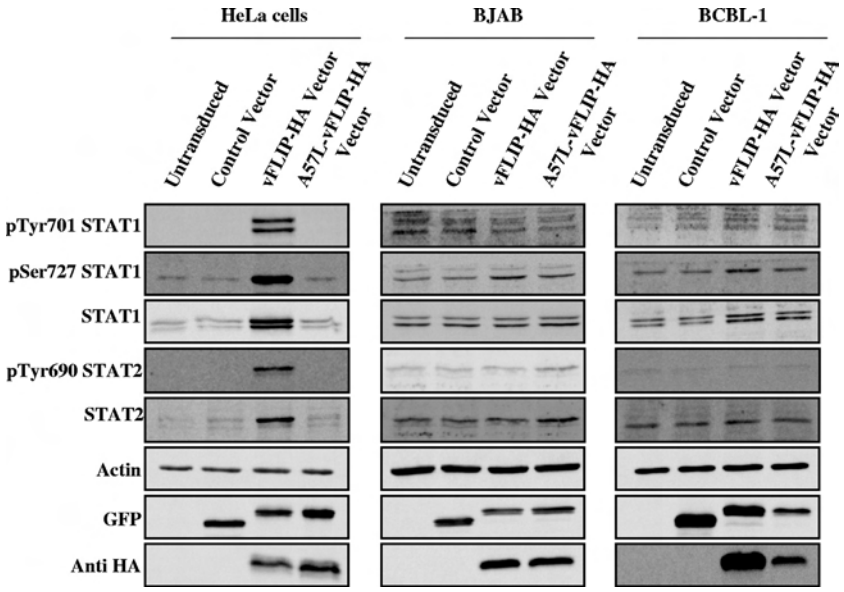

FIG. 8. vFLIP-mediated STAT1 and STAT2 phosphorylation is cell type dependent. The indicated cell lines were transduced with vFLIP-HA-expressing lentivirus, A57L-vFLIP-HA-expressing lentivirus, or the control lentivirus or left untransduced. Cells were lysed 48 h after transduction and checked for the expression of the indicated protein by immunoblotting. See Fig. 7 for an explanation of the bands stained with antibodies to GFP and HA.

this in our study. In contrast, only a few cellular genes were differentially upregulated by vFLIP in the context of the whole virus genome. This could be attributed to the low level of vFLIP expression and indicates the importance of studying the effects of vFLIP in the course of natural infection. Surprisingly, all the cellular genes that were consistently and unidirectionally regulated by vFLIP overexpression and by vFLIP in the context of the whole viral genome in infected endothelial cells are known to be interferon inducible. As vFLIP does not induce the expression of genes encoding type I and II interferon while permitting the phosphorylation of STAT1 and STAT2, and since the vFLIP-induced phosphorylation of STAT1 and STAT2 does not depend on JAK1, JAK2, or Tyk2 (Fig. 7), it is likely that vFLIP activates the expression of these interferon-inducible genes directly, i.e., independently of interferon induction.

Activation of STAT1 and STAT2 by vFLIP requires the recruitment of IKK-γ to vFLIP and activation of the NF-κB pathway, since the A57L mutant did not induce STAT1 and STAT2 phosphorylation and knockdown of IKK-γ or p65 prevented this activation of STAT1/STAT2 (Fig. 7E and F). However, this vFLIP-mediated STAT1/STAT2 phosphorylation seems to be cell type dependent (Fig. 8). vFLIP failed to induce STAT1/STAT2 phosphorylation in HEK293 cells, in addition to the cell types shown in Fig. 8, although it strongly activates an NF-κB reporter plasmid in this cell line (data not shown), indicating its ability to activate the NF-κB pathway in these cells and suggesting that activation of the NF-κB pathway alone by vFLIP is not sufficient to induce STAT1/STAT2 phosphorylation. In keeping with our observation that a subset of interferon-inducible cellular genes is differentially expressed in KSHV-wt- and KSHV-ΔvFLIP-infected endothelial cells (Fig. 5 and 6), we could show increased STAT1/STAT2 phosphorylation in KSHV-wt- and KSHV-vFLIP-R-infected, compared to uninfected and KSHV-ΔvFLIP-infected, endothelial cells (Fig. 9). These differences in STAT1/STAT2 phosphorylation were detectable, although vFLIP expression in the infected endothelial cells was too low to be visible on Western blots (Fig. 9).

Activation of STAT1 and STAT2 by vFLIP may serve the purpose of inducing one or several cellular genes identified in this study as being differentially expressed between KSHV-wt- and KSHV-ΔFLIP-infected cells. Some of these have other functions that fit with properties previously attributed to

FIG. 7. vFLIP upregulates the expression of JAK2, STAT1, and STAT2 and induces the phosphorylation of STAT1 and STAT2 in an NF-κB-dependent manner. (A to D) Primary HUVECs were left untransduced or transduced with a lentiviral vector expressing vFLIP-HA, the NF-κB activation-deficient mutant A57L-vFLIP-HA in the form of a GFP-T2A-vFLIP-HA fusion protein, or the control lentivirus. After 48 h, cells were lysed and tested for JAK1, JAK2, Tyk2, STAT1, and STAT2 expression and phosphorylation. The higher molecular weight of the GFP-reactive band in vFLIP-HA- and A57L-vFLIP-HA-transduced cells is due to the T2A element left bound to GFP after the cotranslational cleavage of vFLIP-HA or A57L-vFLIP-HA from, respectively, the GFP-T2A-vFLIP-HA and GFP-T2A-A57L-vFLIP-HA fusion proteins. vFLIP and A57L-vFLIP expression was detected with an antibody to the HA tag. (C) The positive-control lane represents a lysate from HEK293 cells transfected with a plasmid expressing a constitutive active STAT5 as a positive control. (D) HeLa cells were induced with either 0, 20, or 50 ng/ml of human IL-4 for 15 min and then lysed and used as a positive control. (B) HUVECs (100,000 cells) were transfected with 100 pmol of the indicated siRNA using microporation. Twenty-four hours later, they were transduced with either the vFLIP-expressing vector or its control vector. After 48 h, cell lysates were prepared and analyzed for protein expression.

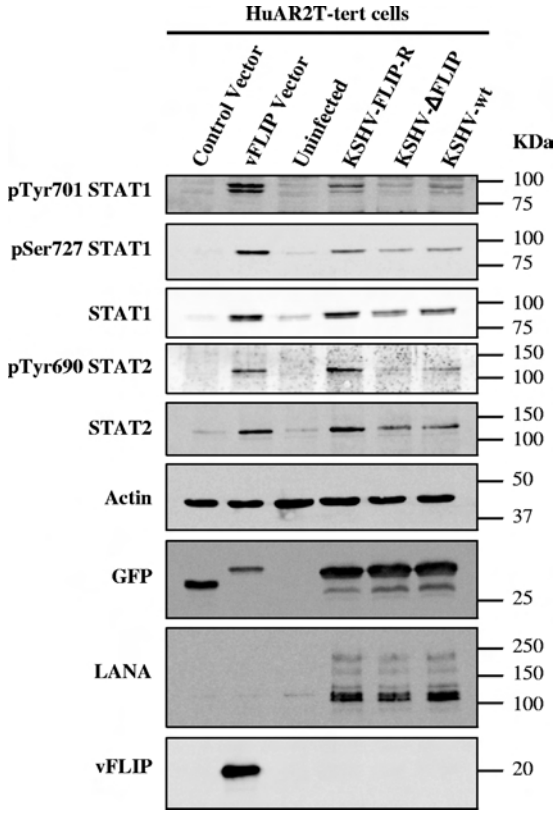

FIG. 9. Conditionally immortalized endothelial cells (HuAR2T-tert) were infected with KSHV-wt, KSHV-ΔFLIP, or KSHV-FLIP-R at an MOI of 1 and selected with hygromycin to generate stable cell lines. Uninfected and stably infected cells (2.5×10^5) were plated in each well of a 6-well plate and 24 h later were washed with PBS and lysed. Cellular lysates were analyzed for STAT1/STAT2 phosphorylation as well as protein expression of STAT1/STAT2, actin, GFP, LANA, and vFLIP by Western blotting. Cellular lysates of vFLIP- or control vector-transduced HuAR2T-tert cells were collected 24 h after transduction and used as a positive control.

vFLIP. IFI6 (G1P3), for example, localizes to mitochondria and inhibits mitochondrion-mediated apoptosis in human myeloma cells and the gastric cancer cell line (16, 62). Thereby, upregulation of IFI6 by vFLIP, in addition to previously reported SOD2 (64), may protect infected cells from mitochondrion-induced apoptosis. IFITM1, among other interferon-inducible genes, is upregulated in Epstein-Barr virus (EBV)-positive monomorphic B cell posttransplant lymphoproliferative disorders (19). The LY6E gene is one of the signature genes in breast cancer metastasizing to lung (46) and was shown to be involved in the self-renewal of erythroid progenitors and to be highly expressed in some human cancers (7). *PARP9* (*BAL1*) was identified as a risk-related gene expressed in diffuse B cell lymphoma (1). Other genes upregulated by vFLIP in infected endothelial cells are reported to have antiviral effects. *BST2*/*tetherin*, for example, inhibits the release of HIV-1 viral particles by tethering them to the cell membrane (49). While HIV-1 uses *vpu* to neutralize the effect of BST2 (39), KSHV expresses K5 upon reactivation of lytic replication to downregulate BST2 and facilitate KSHV virion release (4, 40). In keeping with our results, BST2 expression has previously been reported to be upregulated in E6/E7-immortalized dermal microvascular endothelial cells (DMVEC) latently infected with KSHV (40), indicating a role for this protein during latency.

Although the mouse Mx1 and -2 as well as the human MxA proteins exhibit antiviral activities, the human Mx2 homolog (MxB), upregulated by vFLIP, shows no antiviral functions (25, 47, 48). King et al. have shown that MxB localizes to the cytoplasmic phase of the nuclear pore and that the expression of either GTP-binding- or GTP hydrolysis-defective mutants disrupts nuclear import and significantly delays the progression of the cell cycle from G_0/G_1 into S phase (34).

On the other hand, activation of the interferon response pathway by vFLIP may also contribute to the inhibition of lytic reactivation, since a recent report described that the murine herpesvirus 68 (MHV-68) *orf50*/RTA gene promoter is repressed by gamma interferon and STAT1, implying a role for the interferon response pathway in the control of lytic replication (28). In addition, interferon-independent activation of STAT1 in EBV-infected B cells has been shown to prevent the activation of the lytic replication cycle and to maintain the EBV latency III program in LCL cells (45). Interestingly, the interferon-independent activation of STAT1 in EBV-infected lymphoma or LCL cells occurs in the absence of Tyr 701 phosphorylation (44). Thus, the lack of Tyr 701 phosphorylation in vFLIP-transduced B cells (Fig. 7 and 8) may not preclude an activation of STAT1 by vFLIP in these cells.

A recent study (35) found that the human cytomegalovirus IE1 protein induces STAT1 phosphorylation and elicits a type II interferon-like host cell response involving the selective upregulation of immune-stimulatory genes, including proinflammatory cytokines. Several large DNA viruses may therefore be able to exploit a component of the innate immune response, which is usually known for its antiviral properties, for their own benefit. Further studies are needed to clarify the benefit that activation of a STAT1- and STAT2-dependent pathway by vFLIP affords to KSHV. However, the results reported in this study indicate that the effect of vFLIP on STAT1-dependent cellular genes appears to dominate the difference in cellular gene expression observed between endothelial cells infected with a wild-type and a vFLIP-deleted KSHV.

ACKNOWLEDGMENTS

This work was supported by grants from the Deutsche Forschungsgemeinschaft (DFG; Schu1688-2/3) and EU integrated project INCA (LSHC-CT-2005-018704) to T.F.S. as well as grant DFG-GK1071 and a grant from the Interdisciplinary Center for Clinical Research (IZKF) of the University of Erlangen-Nuremberg to M.S.

We thank Axel Schambach and Renata Stripeke for providing us with the plasmids required for the production of the vFLIP lentivirus.

REFERENCES

1. **Aguiar, R. C., et al.** 2000. BAL is a novel risk-related gene in diffuse large B-cell lymphomas that enhances cellular migration. Blood **96:**4328–4334.
2. **Bagnéris, C., et al.** 2008. Crystal structure of a vFlip-IKKgamma complex: insights into viral activation of the IKK signalosome. Mol. Cell **30:**620–631.
3. **Ballon, G., K. Chen, R. Perez, W. Tam, and E. Cesarman.** 2011. Kaposi sarcoma herpesvirus (KSHV) vFLIP oncoprotein induces B cell transdifferentiation and tumorigenesis in mice. J. Clin. Invest. **121:**1141–1153.
4. **Bartee, E., A. McCormack, and K. Fruh.** 2006. Quantitative membrane proteomics reveals new cellular targets of viral immune modulators. PLoS Pathog. **2:**e107.
5. **Bertin, J., et al.** 1997. Death effector domain-containing herpesvirus and poxvirus proteins inhibit both Fas- and TNFR1-induced apoptosis. Proc. Natl. Acad. Sci. U. S. A. **94:**1172–1176.

6. **Bieleski, L., C. Hindley, and S. J. Talbot.** 2004. A polypyrimidine tract facilitates the expression of Kaposi's sarcoma-associated herpesvirus vFLIP through an internal ribosome entry site. J. Gen. Virol. **85:**615–620.
7. **Bresson-Mazet, C., O. Gandrillon, and S. Gonin-Giraud.** 2008. Stem cell antigen 2: a new gene involved in the self-renewal of erythroid progenitors. Cell Prolif. **41:**726–738.
8. **Brinkmann, M. M., et al.** 2003. Activation of mitogen-activated protein kinase and NF-κB pathways by a Kaposi's sarcoma-associated herpesvirus K15 membrane protein. J. Virol. **77:**9346–9358.
9. **Cai, X., et al.** 2005. Kaposi's sarcoma-associated herpesvirus expresses an array of viral microRNAs in latently infected cells. Proc. Natl. Acad. Sci. U. S. A. **102:**5570–5575.
10. **Cannon, J. S., et al.** 2000. A new primary effusion lymphoma-derived cell line yields a highly infectious Kaposi's sarcoma herpesvirus-containing supernatant. J. Virol. **74:**10187–10193.
11. **Carroll, P. A., E. Brazeau, and M. Lagunoff.** 2004. Kaposi's sarcoma-associated herpesvirus infection of blood endothelial cells induces lymphatic differentiation. Virology **328:**7–18.
12. **Cesarman, E., Y. Chang, P. S. Moore, J. W. Said, and D. M. Knowles.** 1995. Kaposi's sarcoma-associated herpesvirus-like DNA sequences in AIDS-related body-cavity-based lymphomas. N. Engl. J. Med. **332:**1186–1191.
13. **Chandriani, S., and D. Ganem.** 2010. Array-based transcript profiling and limiting-dilution reverse transcription-PCR analysis identify additional latent genes in Kaposi's sarcoma-associated herpesvirus. J. Virol. **84:**5565–5573.
14. **Chang, Y., et al.** 1994. Identification of herpesvirus-like DNA sequences in AIDS-associated Kaposi's sarcoma. Science **266:**1865–1869.
15. **Chaudhary, P. M., A. Jasmin, M. T. Eby, and L. Hood.** 1999. Modulation of the NF-kappa B pathway by virally encoded death effector domains-containing proteins. Oncogene **18:**5738–5746.
16. **Cheriyath, V., et al.** 2007. G1P3, an IFN-induced survival factor, antagonizes TRAIL-induced apoptosis in human myeloma cells. J. Clin. Invest. **117:** 3107–3117.
17. **Chugh, P., et al.** 2005. Constitutive NF-kappaB activation, normal Fas-induced apoptosis, and increased incidence of lymphoma in human herpes virus 8 K13 transgenic mice. Proc. Natl. Acad. Sci. U. S. A. **102:**12885–12890.
18. **Ciufo, D. M., et al.** 2001. Spindle cell conversion by Kaposi's sarcoma-associated herpesvirus: formation of colonies and plaques with mixed lytic and latent gene expression in infected primary dermal microvascular endothelial cell cultures. J. Virol. **75:**5614–5626.
19. **Craig, F. E., et al.** 2007. Gene expression profiling of Epstein-Barr virus-positive and -negative monomorphic B-cell posttransplant lymphoproliferative disorders. Diagn. Mol. Pathol. **16:**158–168.
20. **Datsenko, K. A., and B. L. Wanner.** 2000. One-step inactivation of chromosomal genes in *Escherichia coli* K-12 using PCR products. Proc. Natl. Acad. Sci. U. S. A. **97:**6640–6645.
21. **Efklidou, S., R. Bailey, N. Field, M. Noursadeghi, and M. K. Collins.** 2008. vFLIP from KSHV inhibits anoikis of primary endothelial cells. J. Cell Sci. **121:**450–457.
22. **Emuss, V., et al.** 2009. KSHV manipulates Notch signaling by DLL4 and JAG1 to alter cell cycle genes in lymphatic endothelia. PLoS Pathog. **5:**e1000616.
23. **Field, N., et al.** 2003. KSHV vFLIP binds to IKK-gamma to activate IKK. J. Cell Sci. **116:**3721–3728.
24. **Flore, O., et al.** 1998. Transformation of primary human endothelial cells by Kaposi's sarcoma-associated herpesvirus. Nature **394:**588–592.
25. **Frese, M., G. Kochs, U. Meier-Dieter, J. Siebler, and O. Haller.** 1995. Human MxA protein inhibits tick-borne Thogoto virus but not Dhori virus. J. Virol. **69:**3904–3909.
26. **Gao, S. J., J. H. Deng, and F. C. Zhou.** 2003. Productive lytic replication of a recombinant Kaposi's sarcoma-associated herpesvirus in efficient primary infection of primary human endothelial cells. J. Virol. **77:**9738–9749.
27. **Godfrey, A., J. Anderson, A. Papanastasiou, Y. Takeuchi, and C. Boshoff.** 2005. Inhibiting primary effusion lymphoma by lentiviral vectors encoding short hairpin RNA. Blood **105:**2510–2518.
28. **Goodwin, M. M., S. Canny, A. Steed, and H. W. Virgin.** 2010. Murine gammaherpesvirus 68 has evolved gamma interferon and Stat1-repressible promoters for the lytic switch gene 50. J. Virol. **84:**3711–3717.
29. **Grossmann, C., S. Podgrabinska, M. Skobe, and D. Ganem.** 2006. Activation of NF-κB by the latent vFLIP gene of Kaposi's sarcoma-associated herpesvirus is required for the spindle shape of virus-infected endothelial cells and contributes to their proinflammatory phenotype. J. Virol. **80:**7179–7185.
30. **Grundhoff, A., C. S. Sullivan, and D. Ganem.** 2006. A combined computational and microarray-based approach identifies novel microRNAs encoded by human gamma-herpesviruses. RNA **12:**733–750.
31. **Guasparri, I., S. A. Keller, and E. Cesarman.** 2004. KSHV vFLIP is essential for the survival of infected lymphoma cells. J. Exp. Med. **199:**993–1003.
32. **Hong, Y. K., et al.** 2004. Lymphatic reprogramming of blood vascular endothelium by Kaposi sarcoma-associated herpesvirus. Nat. Genet. **36:**683–685.
33. **Jaffe, E. A., R. L. Nachman, C. G. Becker, and C. R. Minick.** 1973. Culture of human endothelial cells derived from umbilical veins. Identification by morphologic and immunologic criteria. J. Clin. Invest. **52:**2745–2756.
34. **King, M. C., G. Raposo, and M. A. Lemmon.** 2004. Inhibition of nuclear import and cell-cycle progression by mutated forms of the dynamin-like GTPase MxB. Proc. Natl. Acad. Sci. U. S. A. **101:**8957–8962.
35. **Knoblach, T., B. Grandel, J. Seiler, M. Nevels, and C. Paulus.** 2011. Human cytomegalovirus IE1 protein elicits a type II interferon-like host cell response that depends on activated STAT1 but not interferon-γ. PLoS Pathog. **7:**e1002016.
36. **Konrad, A., et al.** 2009. A systems biology approach to identify the combination effects of human herpesvirus 8 genes on NF-κB activation. J. Virol. **83:**2563–2574.
37. **Lei, X., et al.** 2010. Regulation of NF-kappaB inhibitor IkappaBalpha and viral replication by a KSHV microRNA. Nat. Cell Biol. **12:**193–199.
38. **Low, W., et al.** 2001. Internal ribosome entry site regulates translation of Kaposi's sarcoma-associated herpesvirus FLICE inhibitory protein. J. Virol. **75:**2938–2945.
39. **Mangeat, B., et al.** 2009. HIV-1 Vpu neutralizes the antiviral factor tetherin/BST-2 by binding it and directing its beta-TrCP2-dependent degradation. PLoS Pathog. 5:e1000574.
40. **Mansouri, M., et al.** 2009. Molecular mechanism of BST2/tetherin downregulation by K5/MIR2 of Kaposi's sarcoma-associated herpesvirus. J. Virol. **83:**9672–9681.
41. **Matta, H., and P. M. Chaudhary.** 2004. Activation of alternative NF-kappa B pathway by human herpes virus 8-encoded Fas-associated death domain-like IL-1 beta-converting enzyme inhibitory protein (vFLIP). Proc. Natl. Acad. Sci. U. S. A. **101:**9399–9404.
42. **Matta, H., et al.** 2007. Induction of spindle cell morphology in human vascular endothelial cells by human herpesvirus 8-encoded viral FLICE inhibitory protein K13. Oncogene **26:**1656–1660.
43. **May, T., et al.** 2010. Synthetic gene regulation circuits for control of cell expansion. Tissue Eng. Part A **16:**441–452.
44. **McLaren, J., M. Rowe, and P. Brennan.** 2007. Epstein-Barr virus induces a distinct form of DNA-bound STAT1 compared with that found in interferon-stimulated B lymphocytes. J. Gen. Virol. **88:**1876–1886.
45. **McLaren, J. E., et al.** 2009. STAT1 contributes to the maintenance of the latency III viral programme observed in Epstein-Barr virus-transformed B cells and their recognition by CD8+ T cells. J. Gen. Virol. **90:**2239–2250.
46. **Minn, A. J., et al.** 2005. Genes that mediate breast cancer metastasis to lung. Nature **436:**518–524.
47. **Netherton, C. L., et al.** 2009. Inhibition of a large double-stranded DNA virus by MxA protein. J. Virol. **83:**2310–2320.
48. **Pavlovic, J., T. Zurcher, O. Haller, and P. Staeheli.** 1990. Resistance to influenza virus and vesicular stomatitis virus conferred by expression of human MxA protein. J. Virol. **64:**3370–3375.
49. **Perez-Caballero, D., et al.** 2009. Tetherin inhibits HIV-1 release by directly tethering virions to cells. Cell **139:**499–511.
50. **Peter, M. E.** 2004. The flip side of FLIP. Biochem. J. **382:**e1–e3.
51. **Pfeffer, S., et al.** 2005. Identification of microRNAs of the herpesvirus family. Nat. Methods **2:**269–276.
52. **Punj, V., H. Matta, S. Schamus, and P. M. Chaudhary.** 2009. Integrated microarray and multiplex cytokine analyses of Kaposi's sarcoma associated herpesvirus viral FLICE inhibitory protein K13 affected genes and cytokines in human blood vascular endothelial cells. BMC Med. Genomics **2:**50.
53. **Sakakibara, S., C. A. Pise-Masison, J. N. Brady, and G. Tosato.** 2009. Gene regulation and functional alterations induced by Kaposi's sarcoma-associated herpesvirus-encoded ORFK13/vFLIP in endothelial cells. J. Virol. **83:** 2140–2153.
54. **Samaniego, F., S. Pati, J. E. Karp, O. Prakash, and D. Bose.** 2001. Human herpesvirus 8 K1-associated nuclear factor-kappa B-dependent promoter activity: role in Kaposi's sarcoma inflammation? J. Natl. Cancer Inst. Monogr. **28:**15–23.
55. **Samols, M. A., J. Hu, R. L. Skalsky, and R. Renne.** 2005. Cloning and identification of a microRNA cluster within the latency-associated region of Kaposi's sarcoma-associated herpesvirus. J. Virol. **79:**9301–9305.
56. **Schulz, T. F.** 2006. The pleiotropic effects of Kaposi's sarcoma herpesvirus. J. Pathol. **208:**187–198.
57. **Soulier, J., et al.** 1995. Kaposi's sarcoma-associated herpesvirus-like DNA sequences in multicentric Castleman's disease. Blood **86:**1276–1280.
58. **Stürzl, M., et al.** 1999. Expression of K13/v-FLIP gene of human herpesvirus 8 and apoptosis in Kaposi's sarcoma spindle cells. J. Natl. Cancer Inst. **91:**1725–1733.
59. **Sullivan, C. S., A. T. Grundhoff, S. Tevethia, J. M. Pipas, and D. Ganem.** 2005. SV40-encoded microRNAs regulate viral gene expression and reduce susceptibility to cytotoxic T cells. Nature **435:**682–686.
60. **Sun, Q., H. Matta, G. Lu, and P. M. Chaudhary.** 2006. Induction of IL-8 expression by human herpesvirus 8 encoded vFLIP K13 via NF-kappaB activation. Oncogene **25:**2717–2726.
61. **Sun, Q., S. Zachariah, and P. M. Chaudhary.** 2003. The human herpes virus 8-encoded viral FLICE-inhibitory protein induces cellular transformation via NF-kappaB activation. J. Biol. Chem. **278:**52437–52445.
62. **Tahara, E., Jr., et al.** 2005. G1P3, an interferon inducible gene 6-16, is expressed in gastric cancers and inhibits mitochondrial-mediated apoptosis in gastric cancer cell line TMK-1 cell. Cancer Immunol. Immunother. **54:** 729–740.

63. **Thome, M., et al.** 1997. Viral FLICE-inhibitory proteins (FLIPs) prevent apoptosis induced by death receptors. Nature **386:**517–521.
64. **Thurau, M., et al.** 2009. Viral inhibitor of apoptosis vFLIP/K13 protects endothelial cells against superoxide-induced cell death. J. Virol. **83:**598–611.
65. **Tischer, B. K., J. von Einem, B. Kaufer, and N. Osterrieder.** 2006. Two-step red-mediated recombination for versatile high-efficiency markerless DNA manipulation in *Escherichia coli*. Biotechniques **40:**191–197.
66. **Vieira, J., and P. M. O'Hearn.** 2004. Use of the red fluorescent protein as a marker of Kaposi's sarcoma-associated herpesvirus lytic gene expression. Virology **325:**225–240.
67. **Wang, H. W., et al.** 2004. Kaposi sarcoma herpesvirus-induced cellular reprogramming contributes to the lymphatic endothelial gene expression in Kaposi sarcoma. Nat. Genet. **36:**687–693.
68. **Wang, L., et al.** 2007. Functional characterization of the M-type K15-encoded membrane protein of Kaposi's sarcoma-associated herpesvirus. J. Gen. Virol. **88:**1698–1707.
69. **Wang, L., and B. Damania.** 2008. Kaposi's sarcoma-associated herpesvirus confers a survival advantage to endothelial cells. Cancer Res. **68:**4640–4648.
70. **Xu, Y., and D. Ganem.** 2007. Induction of chemokine production by latent Kaposi's sarcoma-associated herpesvirus infection of endothelial cells. J. Gen. Virol. **88:**46–50.
71. **Ye, F. C., et al.** 2008. Kaposi's sarcoma-associated herpesvirus latent gene vFLIP inhibits viral lytic replication through NF-κB-mediated suppression of the AP-1 pathway: a novel mechanism of virus control of latency. J. Virol. **82:**4235–4249.
72. **Zhao, J., et al.** 2007. K13 blocks KSHV lytic replication and deregulates vIL6 and hIL6 expression: a model of lytic replication induced clonal selection in viral oncogenesis. PLoS One **2:**e1067.
73. **Zhou, F. C., et al.** 2002. Efficient infection by a recombinant Kaposi's sarcoma-associated herpesvirus cloned in a bacterial artificial chromosome: application for genetic analysis. J. Virol. **76:**6185–6196.